

Nanometer structural columns and frustration of magnetic ordering in $\text{Nb}_{12}\text{O}_{29}$ E. N. Andersen,¹ T. Klimczuk,^{1,2} V. L. Miller,¹ H. W. Zandbergen,³ and R. J. Cava¹¹Department of Chemistry, Princeton University, Princeton, New Jersey 08544, USA²Faculty of Applied Physics and Mathematics, Gdansk University of Technology, Narutowicza 11/12, 80-952 Gdansk, Poland³National Center for HREM, Department of Nanoscience, Delft University of Technology, Rotterdamseweg 137, 2682 AL Delft, The Netherlands

(Received 1 April 2005; published 22 July 2005)

Single phase samples of the monoclinic and orthorhombic polymorphs of $\text{Nb}_{12}\text{O}_{29}$ have been identified and isolated. These polymorphs have different arrangements of nanometer dimension structural columns of ReO_3 -type niobium oxygen arrays: They differ in structure after a 3-nm translation in one of three dimensions while being the same in the other two. Magnetic susceptibility measurements show that one polymorph displays an antiferromagnetic transition at 12 K, along with short-range order fluctuations up to 25 K, while the other shows strict Curie-Weiss behavior down to 2 K.

DOI: 10.1103/PhysRevB.72.033413

PACS number(s): 75.20.Hr, 61.66.Fn, 75.50.Ee, 81.05.Je

$\text{Nb}_{12}\text{O}_{29}$, one of the rare compounds in which Nb displays a local magnetic moment, is also one of the small number of transition metal oxides that shows both antiferromagnetic ordering and metallic conductivity at low temperatures.^{1,2} When these properties do coexist, as in $\text{Na}_{0.7}\text{CoO}_2$, correlated electron physics is often the cause.³⁻⁵ $\text{Nb}_{12}\text{O}_{29}$ adds an additional degree of structural complexity to the study of electronic and magnetic properties of materials. This compound displays two structural variants that differ due to the arrangement of structural building blocks on the nanometer-length scale. Here we show that although the local magnetic and structural characteristics are similar for both structures, one variant magnetically orders at 12 K while the other does not. Because the long-range ordering of magnetic moments at low temperatures is dominated by interactions on the angstrom scale, the effect of the nanometer scale structural ar-

angement on the magnetic properties of $\text{Nb}_{12}\text{O}_{29}$ is unexpected.

$\text{Nb}_{12}\text{O}_{29}$ displays a crystallographic shear structure. Such structures are based on an oxygen-deficient ReO_3 -type lattice, with the oxygen deficiency accommodated by a complete structural rearrangement—a “shearing” of the ReO_3 network to create planes of edge-shared MO_6 octahedra with a lower oxygen to metal ratio. In niobium oxide shear structures, the presence of two intersecting shear planes leads to the formation of nanometer-size ReO_3 -like columns, yielding distinct, fully ordered crystal structures for the formulas Nb_2O_5 , $\text{Nb}_{53}\text{O}_{132}$, $\text{Nb}_{22}\text{O}_{54}$, $\text{Nb}_{25}\text{O}_{62}$, $\text{Nb}_{47}\text{O}_{116}$, and $\text{Nb}_{12}\text{O}_{29}$.⁶

Orthorhombic and monoclinic forms of $\text{Nb}_{12}\text{O}_{29}$ have been reported.⁷⁻¹⁰ Both forms (Fig. 1) are composed of corner-shared NbO_6 octahedra arranged in ReO_3 -type col-

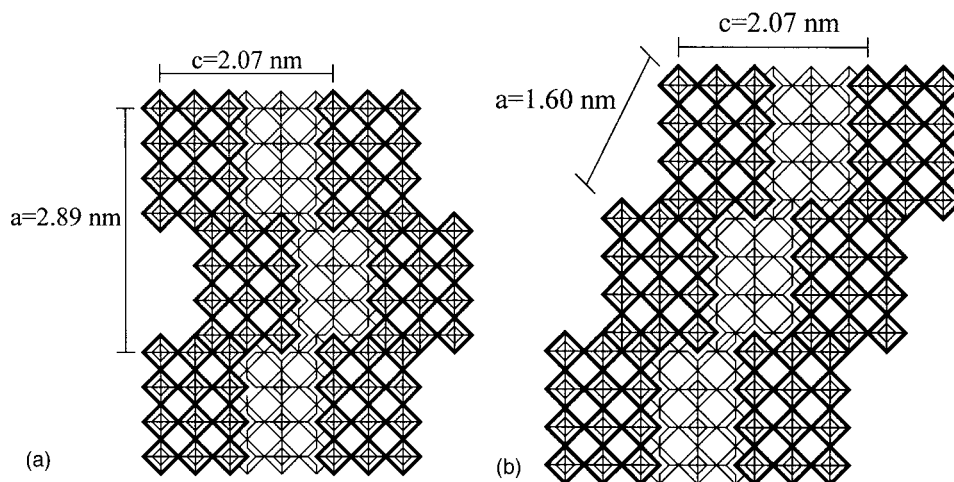


FIG. 1. (a) The idealized crystal structure of orthorhombic $\text{Nb}_{12}\text{O}_{29}$. Space group $Amma$, cell parameters $a=28.90$, $b=3.83$, $c=20.729$ (Ref. 7). (b) The idealized crystal structure of monoclinic $\text{Nb}_{12}\text{O}_{29}$. Space group $A2/a$, cell parameters $a=15.9856$, $b=3.832$, $c=20.720$, $\beta=112.93^\circ$ (Refs. 8 and 10). The NbO_6 octahedra are shown as geometric figures. The bold columns of corner shared NbO_6 octahedra are at the same elevation perpendicular to the plane of the paper. The lighter columns are displaced by $1/2$ an octahedron perpendicular to plane of paper such that they share edges with the bold columns where they touch. The real structures are not formed by perfectly regular octahedra, but instead have some asymmetric bond lengths and angles.

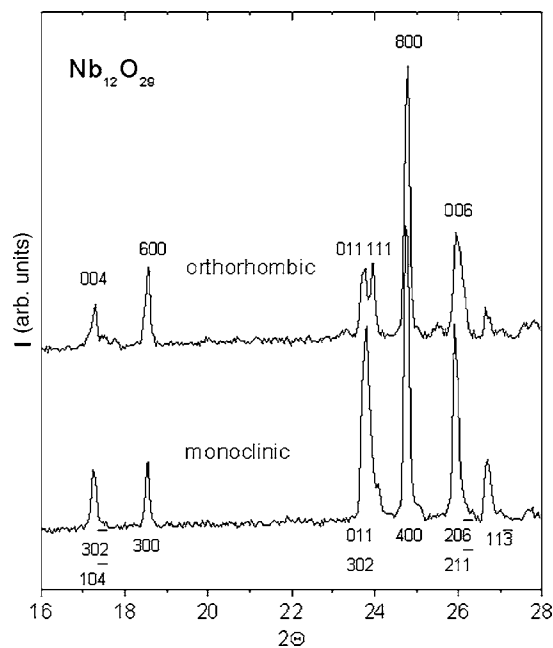


FIG. 2. The characteristic region of the x-ray powder diffraction patterns of $\text{Nb}_{12}\text{O}_{29}$ in the monoclinic and orthorhombic forms. (Cu $K\alpha$ radiation, Si internal standard)

umns that are infinite in extent in one dimension (the b axis), but only 3-octahedra long by 4-octahedra wide in the other two dimensions. The octahedra are approximately 0.4 nm across, making the columns 1.2×1.6 nm in cross section. As shown in Fig. 1, the pattern of edge sharing among these columns differentiates the two forms. In the orthorhombic form, an orthogonal cell is found because columns share *cis* corners with columns at the same level. In the monoclinic form, the columns share *trans* corners. Both within the columns, and where they join, the arrangements of the octahedra are the same in both variants. In addition, the arrangement of near-neighbor columns in the characteristic plane (the plane of Fig. 1) is identical for the two structures. The rearrangement of the columns on going from the monoclinic to the orthorhombic form has two effects, both long range and local: on the nanometer scale, the structures differ only after about a 3-nm translation in one of their three dimensions; on the angstrom scale, the symmetry of the crystal structures has changed. Most importantly, a mirror plane per-

pendicular to the plane of Fig. 1 is missing in the monoclinic form, and all local symmetries are correspondingly lowered.

Synthesis of pure bulk samples of orthorhombic and monoclinic $\text{Nb}_{12}\text{O}_{29}$ is complicated by the robustness of the orthorhombic form.¹¹ Synthesis of monoclinic $\text{Nb}_{12}\text{O}_{29}$ has been reported for temperatures between 1000 and 1200 °C.⁷⁻¹⁰ We confirmed that pure phase monoclinic $\text{Nb}_{12}\text{O}_{29}$ can be synthesized at 1200 °C, and found that pure phase orthorhombic $\text{Nb}_{12}\text{O}_{29}$ was formed at temperatures above 1400 °C. We also found that the orthorhombic phase remained present in small proportion in samples heated briefly at 1400 °C, even if such samples were later annealed for long times at temperatures where the monoclinic phase is stable.

All samples were made from stoichiometric amounts of Nb_2O_5 (Aldrich, 99.99% purity) and NbO_2 (Johnson-Matthey, 99+% purity), mixed and ground until homogeneous. Samples were pelleted and wrapped in Molybdenum foil. Monoclinic $\text{Nb}_{12}\text{O}_{29}$ was obtained by heating the wrapped pellets in an alumina crucible at 1200 °C for 60 h. Orthorhombic $\text{Nb}_{12}\text{O}_{29}$ was obtained by heating the wrapped pellets in a zirconia crucible for 24 h at 1400 °C. A mixed-phase sample was prepared by heating a sample in an alumina crucible for 12 min at 1400 °C and then annealing at 1200 °C for 48 h. All samples were heated in a vacuum furnace, at pressures between 10^{-7} and 10^{-8} Torr.

The standard method for phase identification in oxide systems is powder x-ray diffraction. However, the fact that the Nb_nO_m crystallographic shear structures differ primarily at the nanometer scale complicates the interpretation of such patterns. The low angle, large interplanar spacing regions are the most characteristic. The powder x-ray diffraction patterns between 16° and $28^\circ 2\theta$ (Cu $K\alpha$ radiation, Si internal standard) for the orthorhombic and monoclinic forms of $\text{Nb}_{12}\text{O}_{29}$ prepared in this study are shown in Fig. 2. The differences are quite minor. Initial distinction between the $\text{Nb}_{12}\text{O}_{29}$ phases was made through careful examination of these patterns. It was necessary, however, to employ electron diffraction and structure imaging to unambiguously identify the phase present and interpret the diffraction patterns.

Electron diffraction and imaging experiments were performed at room temperature with a Philips CM200ST electron microscope equipped with a field emission gun. Electron diffraction was performed using a condenser aperture of 10 μm and an electron probe size of 10-nm diam. Electron

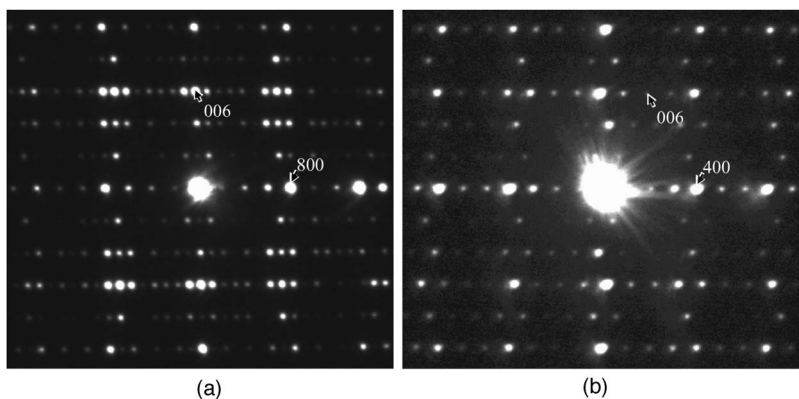


FIG. 3. Electron diffraction patterns in the a - c plane of $\text{Nb}_{12}\text{O}_{29}$ in the two different forms. (a) the orthorhombic form, from a sample synthesized at 1400 °C, (b) the monoclinic form, from the sample synthesized at 1200 °C.

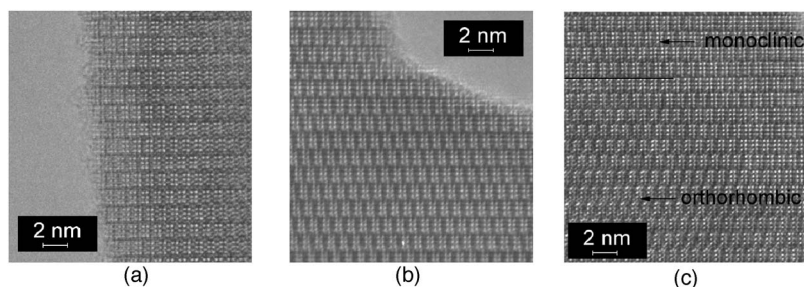


FIG. 4. Structural images of the two forms of $\text{Nb}_{12}\text{O}_{29}$, looking down the short crystallographic b axes. (a) The monoclinic form, from the sample synthesized at 1200 °C, (b) the orthorhombic form, synthesized at 1400 °C, and (c) the mixed phase sample, made by pulsing to 1400 °C and then annealing at 1200 °C.

transparent samples were obtained by crushing the specimens under hexane, and depositing a few droplets on a holey carbon Cu grid. Two types of characteristic electron diffraction patterns (Fig. 3), corresponding to the orthorhombic and monoclinic forms of $\text{Nb}_{12}\text{O}_{29}$, were observed from the samples heated at 1400 and 1200 °C, respectively. Representative strong diffraction peaks are labeled in Fig. 3 from which the relationship between the cells can be seen.

Structures can be unambiguously assigned based on the structural images obtained from the electron diffraction patterns (Fig. 4). The contrast in the images is such that the “holes” between the corner-shared NbO_6 octahedra in the columns appear as white dots in the images. Each 4×3 block of octahedra therefore yields a corresponding 3×2 block of holes, (white dots in the images). The pattern of white dots expected for the different phases can be determined by inspecting Fig. 1 and considering the positions of the holes between octahedra in the columns perpendicular to the plane of the drawing (both bold and ordinary line width columns in Fig. 1 yield equivalent white dot contrast in the electron microscope (EM) images). In addition, in the monoclinic phase, the repeat motif of the 3×2 pattern of dots does not contain a 90° angle, whereas for the orthorhombic phase it does (Fig. 4). The structural images therefore clearly indicate that the sample prepared at 1200 °C is a pure monoclinic phase [Fig. 4(b)], while a pure orthorhombic phase is formed at 1400 °C [Fig. 4(a)]. The sample prepared by heating briefly at 1400 °C and then annealing at 1200 °C contains large regions of both the orthorhombic and monoclinic phases, indicating that annealing at 1200 °C does not destroy the orthorhombic phase [Fig. 4(c)]. In the pure orthorhombic and monoclinic samples, the phases were ordered over long distances and showed no signs of intergrowth with other shear structures or with each other.

From a formal valence, localized charge point of view, $\text{Nb}_{12}\text{O}_{29}$ can be considered as $\text{Nb}^{4+}_2\text{Nb}^{5+}_{10}\text{O}_{29}$. Nb^{5+} has no spin, and if the d electrons from the Nb^{4+} were localized, then there would be two spin $\frac{1}{2}$ expected per formula unit. All studies have found a moment consistent with only one spin $\frac{1}{2}$ per formula unit, however, and, metallic conductivity is observed, making $\text{Nb}_{12}\text{O}_{29}$ a rare case of an antiferromagnetic metal, and indicating further that a localized charge point of view (i.e., yielding an insulator) cannot be accurate for this compound. The original reports identified the antiferromagnetically ordered phase ($T_n=12$ K) as being orthorhombic $\text{Nb}_{12}\text{O}_{29}$.^{1,12} More recent studies have reported that the monoclinic phase antiferromagnetically orders at 12 K,¹⁰ but have not confirmed the presence of ordering in the orthorhombic phase. The current paper resolves this discrepancy.

The magnetic susceptibilities of pure phase samples of orthorhombic and monoclinic $\text{Nb}_{12}\text{O}_{29}$, and the one in which the two forms were mixed, were measured on heating from 2–250 K (zero-field cooled) in a field of 10 kOe. We present the magnetic data for the orthorhombic, monoclinic, and mixed samples in Fig. 5. The monoclinic form, with *trans* nanometer column arrangement, orders antiferromagnetically at 12 K (main panel). The orthorhombic form, with a *cis* nanometer column arrangement, shows no such ordering down to 1.8 K. In the mixed sample, the decrease in susceptibility below the ordering temperature is less pronounced, consistent with the presence of some nonordering orthorhombic material. χ is very similar for all three samples above 40 K. The $1/\chi$ inset to Fig. 5 shows the Curie-Weiss behavior for all samples over a broad temperature range. For monoclinic $\text{Nb}_{12}\text{O}_{29}$, $\theta_{\text{CW}}=-27$ K and an effective moment of $1.7\mu_B$ per formula unit are found. In the orthorhombic phase, $\theta_{\text{CW}}=-14$ K and an effective moment of $1.6\mu_B$ per formula unit are found. These moments are consistent with those previously reported,^{1,9–12} at about one spin $\frac{1}{2}$ per $\text{Nb}_{12}\text{O}_{29}$ formula unit. Magnetization versus applied field curves were measured on the three samples at 2, 40, and 100 K (data not shown). All curves were linear up to applied fields of 70 kOe.

How can the fact that antiferromagnetic ordering is

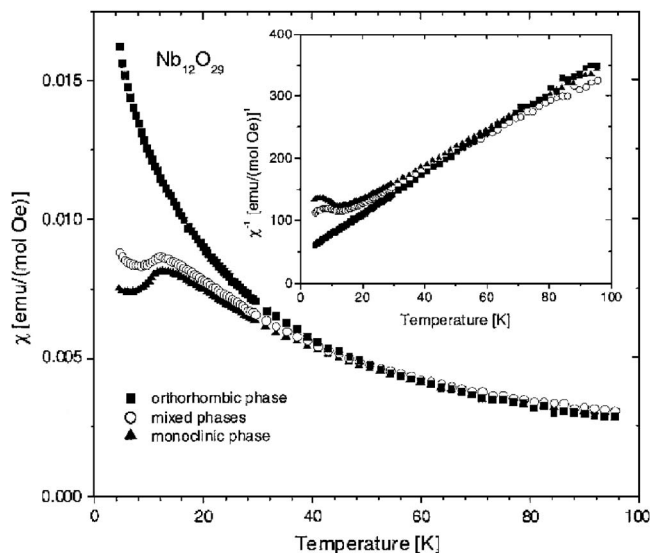


FIG. 5. Magnetic susceptibility below 100 K for the two forms of $\text{Nb}_{12}\text{O}_{29}$ and the sample that is a mixture of the two forms. Main panel: detail of the region in the vicinity of the transition. Inset: inverse susceptibility vs temperature.

present at 12 K for monoclinic Nb₁₂O₂₉ but is suppressed for orthorhombic Nb₁₂O₂₉ be related to the arrangement of the nanometer size structural columns? We offer two possibilities. In a “localized spin” scenario, the single spin $\frac{1}{2}$ magnetic moment per formula unit is localized on one of the symmetry independent Nb ions in each of the complex cells.¹⁰ The other Nb⁴⁺ formally present then has its charge fully delocalized, leading to the conductivity.¹³ Alternatively, it may be that the moments are broadly but unevenly distributed within the columns, a partially localized picture that may remedy difficulties in associating the one localized spin per formula unit with one specific Nb site. In either of these cases, the change of symmetry on rearranging the columns could frustrate the magnetic ordering: The higher symmetry of the orthorhombic form could lead to geometric frustration by allowing closer competition between antiferromagnetically coupled spins on a nearly equilateral triangular sublattice within the orthorhombic structure. Inspection of the structure, however, does not suggest the presence of a triangular sublattice. We note that Fig. 5 shows that the susceptibility of the monoclinic form deviates from the high temperature Curie-Weiss law starting at approximately 25 K, indicating that short-range ordering begins to set in at that

temperature. The fact that the orthorhombic form maintains Curie Weiss behavior to 2 K therefore indicates a strong frustration effect. The nanometer scale structural components in these materials result in electronic structures that consist of many overlapping bands. The electrons at the Fermi energy are near the very bottom of a complex, many electron band dominated by Nb *4d* states. Subtleties in the band structures could give rise to both the unexpected magnetic moments and the conductivity, due to the simultaneous presence of both hybridized and localized states near the Fermi energy. In the second scenario, since antiferromagnetism is unexpected in the first place in such systems as this, it could be that unconventional physics is the underlying cause. Due to the complexity of the electronic states, a competing electronic ground state may be arising in orthorhombic Nb₁₂O₂₉ to suppress the ordering seen in the monoclinic form. Studies of orthorhombic Nb₁₂O₂₉ at temperatures below 2 K would be of interest to determine what that state might be.

The work at Princeton University was supported by NSF Grant No. DMR-0244254, and DOE Grant No. DE-FG02-98-ER45706.

¹R. J. Cava, B. Batlogg, J. J. Krajewski, P. Gammel, H. F. Poulsen, W. F. Peck, Jr., and L. W. Rupp, *Nature (London)* **350**, 598 (1991).

²C. H. Rüsher and M. Nygren, *J. Phys.: Condens. Matter* **3**, 3997 (1991).

³Yayu Wang, Nyrisa Rogado, R. J. Cava, and N. P. Ong, *Nature (London)* **423**, 425 (2003).

⁴I. Terasaki, Y. Sasago, and K. Uchinokura, *Phys. Rev. B* **56**, R12685 (1997).

⁵Y. Ando, N. Miyamoto, K. Segawa, T. Kawata, and I. Terasaki, *Phys. Rev. B* **60**, 10580 (1999).

⁶R. S. Roth, *Prog. Solid State Chem.* **13**, 159 (1980).

⁷R. Norin, *Acta Chem. Scand.* (1947-1973) **17**, 1391 (1963).

⁸R. Norin, M. Carlsson, and B. Elquist, *Acta Chem. Scand.* (1947-

1973) **20**, 871 (1966).

⁹J. E. L. Waldron, M. A. Green, and D. A. Neumann, *J. Am. Chem. Soc.* **123**, 5833 (2001).

¹⁰J. E. L. Waldron, M. A. Green, and D. A. Neumann, *J. Phys. Chem. Solids* **65**, 79 (2004).

¹¹J. E. L. Waldron and M. A. Green in *Solid State Chemistry of Inorganic Materials III*, edited by M. J. Geselbracht, J. Greedan, D. C. Johnson, and M. A. Subramanian, MRS Symposia Proceedings No. 658, (Materials Research Society, Pittsburgh, 2001).

¹²R. J. Cava, B. Batlogg, J. J. Krajewski, H. F. Poulsen, P. Gammel, W. F. Peck, and L. W. Rupp, *Phys. Rev. B* **44**, 6973 (1991).

¹³M. Llundell, P. Alemany, and E. Canadell, *J. Solid State Chem.* **149**, 176 (2000).